IMMUNOLOGY

Self-assembled cGAMP-STINGΔTM signaling complex as a bioinspired platform for cGAMP delivery

Yanpu He[1,2], Celestine Hong[1,2], Emily Z. Yan[1,2], Samantha J. Fletcher[1,2], Ge Zhu[3], Mengdi Yang[3], Yingzhong Li[1,4], Xin Sun[3], Darrell J. Irvine[1,4,5,6], Jiahe Li[3]*, Paula T. Hammond[1,2]*

The stimulator of interferon (IFN) genes (STING) pathway constitutes a highly important part of immune responses against various cancers and infections. Consequently, administration of STING agonists such as cyclic GMP-AMP (cGAMP) has been identified as a promising approach to target these diseases. In cancer cells, STING signaling is frequently impaired by epigenetic silencing of STING; hence, conventional delivery of only its agonist cGAMP may be insufficient to trigger STING signaling. In this work, while expression of STING lacking the transmembrane (TM) domain is known to be unresponsive to STING agonists and is dominant negative when coexpressed with the full-length STING inside cells, we observed that the recombinant TM-deficient STING protein complexed with cGAMP could effectively trigger STING signaling when delivered in vitro and in vivo, including in STING-deficient cell lines. Thus, this bioinspired method using TM-deficient STING may present a universally applicable platform for cGAMP delivery.

INTRODUCTION

Cytosolic detection of pathogen- and cancer cell–derived DNA is a major mechanism for immune clearance by inducing type I interferons (IFNs), and the stimulator of IFN genes (STING) is a master regulator that connects DNA sensing via cyclic guanosine monophosphate (GMP)–adenosine monophosphate (AMP) synthase (cGAS) to IFN induction. As a transmembrane (TM) protein localized to the endoplasmic reticulum (ER), STING consists of an N-terminal TM domain and a C-terminal domain (CTD), the latter of which binds STING agonists [i.e., cyclic dinucleotides (CDNs) such as 2'3' cyclic GMP-AMP (cGAMP)] and downstream signaling protein tank-binding kinase 1 (TBK1) (1). In addition to antibacterial and antiviral infections, recent evidence has shown an important role of STING in generating a spontaneous antitumor T cell response in the tumor microenvironment (TME) (2, 3). Activation of the STING pathway in the TME can augment dendritic cell maturation and the production of type I IFNs and other cytokines, which elicit robust antitumor T cell responses and overcome resistance against immunosuppressive cells that inhibit antitumor immunity (4). These findings have motivated extensive investigations on the delivery of cGAMP as a strategy for cancer immunotherapy (5).

Several key challenges to cGAMP delivery stem from the molecular nature of cGAMP: As a negatively charged small molecule, it is difficult to deliver it to the cytoplasm where STING is located. Moreover, cGAMP is rapidly cleared in vivo, and thus, has limited access to tumors (4, 6, 7). Hence, existing efforts in delivering exogenous cGAMP have focused mostly on the development of novel biomaterials to improve cGAMP's bioavailability. However, one requirement for conventional cGAMP delivery to activate STING signaling is that the cell needs to have functional STING protein. Studies have shown that in cancer cells, STING signaling is frequently impaired because of epigenetic silencing of either STING or cGAS (8, 9). In addition, it is still under debate whether all human populations are responsive to treatments of direct cGAMP administration. The human TMEM173 gene encoding for STING has high heterogeneity, approximately 19% of humans carry the HAQ STING variant (with three amino acid substitutions R71H-G230A-R293Q, hence the acronym HAQ). Recent literature has shown this mutation to be a null allele, resulting in substantial reduction in IFN-β expression (10–14), although some other studies argue that HAQ STING is actually functionally responsive (15, 16).

Here, we developed a universal cGAMP delivery platform that can trigger STING signaling independent of endogenous STING functionality to fully address cells that are STING defective or deficient in humans due to either genetic heterogeneity or cancer. Previous studies have demonstrated that TM domain–deficient STING is capable of activating IFN regulatory factor 3 (IRF3) in cytosolic extracts (17), while others have noted that the TM domain is essential for intracellular STING activation by mediating its translocation from the ER to the Golgi apparatus, where it forms punctate structures indicative of oligomerization (1). This oligomerization—in particular, the formation of well-defined tetrameric or higher-order oligomeric structures—has been demonstrated to be essential to the STING signaling pathway by enabling TBK1 activation, which results in IRF3 binding and phosphorylation (18). While studies have observed a small fraction of cytosolic STING to aggregate upon the addition of cGAMP, the oligomerization of full-length STING is predicted to occur more favorably at high local concentrations on two-dimensional membranes (19, 20). Unexpectedly, by titrating the amount of cGAMP to recombinant, TM domain–deficient STING (STINGΔTM) of ~30 kDa, we observed a near-complete shift in population toward a ~120 kDa–molecular weight ribonucleoprotein complex, suggesting a cGAMP-induced tetramerization. Furthermore, we assessed the functionality of this ribonucleoprotein and found it not only capable of augmenting type I IFN production in cells with endogenous STING expression but also fully activating

[1]Koch Institute for Integrative Cancer Research, Massachusetts Institute of Technology, Cambridge, MA 02139, USA. [2]Department of Chemical Engineering, Massachusetts Institute of Technology, Cambridge, MA 02139, USA. [3]Department of Biological Engineering, Northeastern University, Boston, MA 02115, USA. [4]Department of Biological Engineering, Massachusetts Institute of Technology, Cambridge, MA 02139, USA. [5]Department of Materials Science and Engineering, Massachusetts Institute of Technology, Cambridge, MA 02139, USA. [6]Howard Hughes Medical Institute, Chevy Chase, MD 20815, USA.
*Corresponding author. Email: jiah.li@northeastern.edu (J.L.); hammond@mit.edu (P.T.H.)

type I IFN in STING-defective and even STING-deficient cell lines. Last, we exploited its application with in vivo vaccination studies and observed enhancement of both innate and adaptive immune responses, including the augmentation of type I IFN expression in vitro and of both tumor necrosis factor–α (TNF-α) and IFN-γ in vivo, robust antigen-specific T cell activation and antibody production, and significantly improved therapeutic efficiency in a prophylactic study with melanoma and a treatment study with colon cancer mouse models.

RESULTS
Overview of cGAMP delivery strategies
Most, if not all, existing strategies of STING agonist delivery involve directly encapsulating cGAMP into synthetic delivery vehicles, such as liposomes or polymersomes (Fig. 1A). The primary roles of the vehicles are to package the CDN, modulate cellular uptake, and facilitate endosomal escape (4, 6, 21). The vehicles themselves play no functional role in enabling STING signaling and, thus, can potentially result in decreased efficacy when treating cells with HAQ STING variants or cells deficient in endogenous STING. Consequently, we devised a bioinspired codelivery method that precludes the need for fully functional endogenous STING or cGAMP release from a vehicle, using a recombinant TM domain–deficient STING protein as a high-affinity, stable carrier [K_d ~73 nM (22)] for cGAMP. Furthermore, while preassembling STINGΔTM with cGAMP, we observed that this ribonucleoprotein complex is, in turn, able to tetramerize in response to cGAMP binding to STINGΔTM, forming the essential structure for TBK1 recruitment and downstream signaling (Fig. 1B).

cGAMP binding induces near-complete self-assembly of STINGΔTM into tetramers
To characterize the interaction between cGAMP and STINGΔTM protein, we performed fast protein liquid chromatography (FPLC) analyses in phosphate-buffered saline (PBS) and observed that STINGΔTM without cGAMP predominantly exist as dimers with an estimated molecular weight of 60 kDa (Fig. 2A). We titrated STINGΔTM protein with various molar ratios of cGAMP, incubated the mixture to reach equilibrium, and then injected the mixture through FPLC. While increasing the molar ratio of cGAMP: STINGΔTM, we observed the original STINGΔTM dimer population gradually shifting toward another well-defined population with an estimated molecular weight of 120 kDa, suggesting a transition to a tetrameric conformation. No free cGAMP was eluted from FPLC when STINGΔTM were mixed at less than 0.5 molar equivalence of cGAMP. It was only after cGAMP had tetramerized all STINGΔTM did it start to elute as free cGAMP (Fig. 2, A and C). We also observed with transmission electron microscopy (TEM) that STINGΔTM alone in PBS exists as particles ~14 nm in diameter, and when mixed with cGAMP, the particle diameters approximately doubled to ~29 nm, suggesting the formation of side-by-side tetrameric structures (fig. S1). To verify the role of cGAMP binding in inducing this tetramer self-assembly, we generated mutant STINGΔTM proteins R237A/Y239A for mouse STING and R238A/Y240A for human STING, known to abolish the cGAMP binding capability of STING protein (20). As shown in Fig. 2 (B and D), STINGΔTM R237A/Y239A showed a partially tetrameric structure independent of cGAMP but no further self-assembly with increasing amounts of cGAMP titrated. All cGAMP added eluted as free cGAMP.
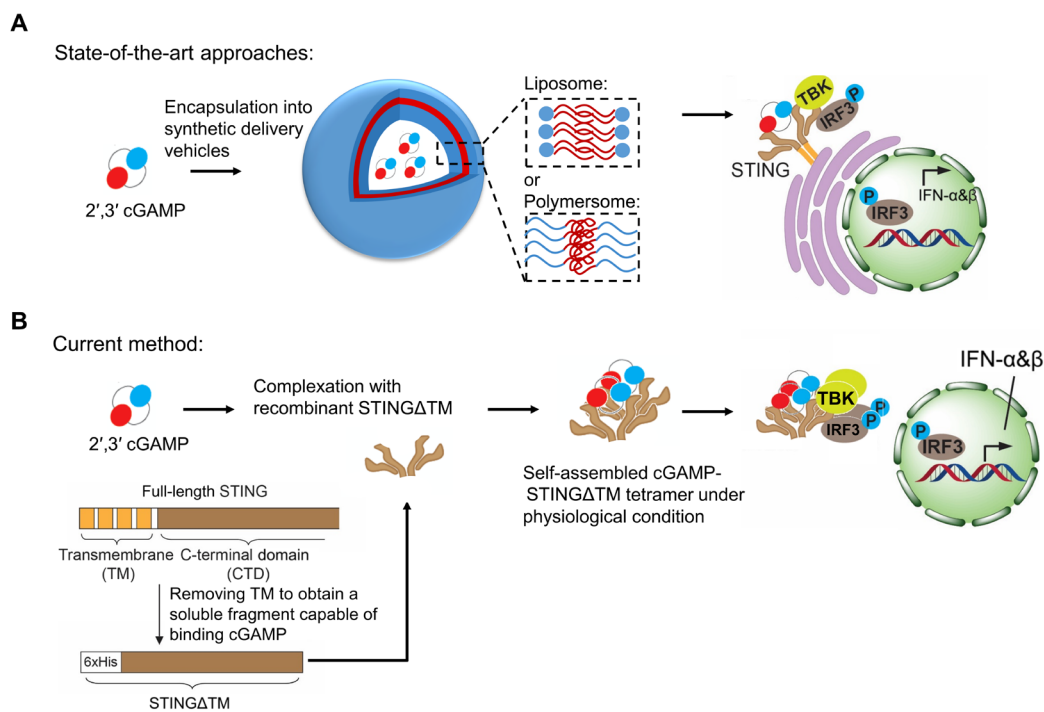

Fig. 1. Overview of state-of-the-art approaches of cGAMP delivery and schematics of recombinant STINGΔTM structure and therapeutic strategy. (A) State-of-the-art approaches through directly encapsulating cGAMP into liposomes or polymersomes for cell transfection. (**B**) Current strategy of delivering cGAMP with a recombinant, transmembrane-deficient STING as carrier in the form of a ribonucleoprotein complex.
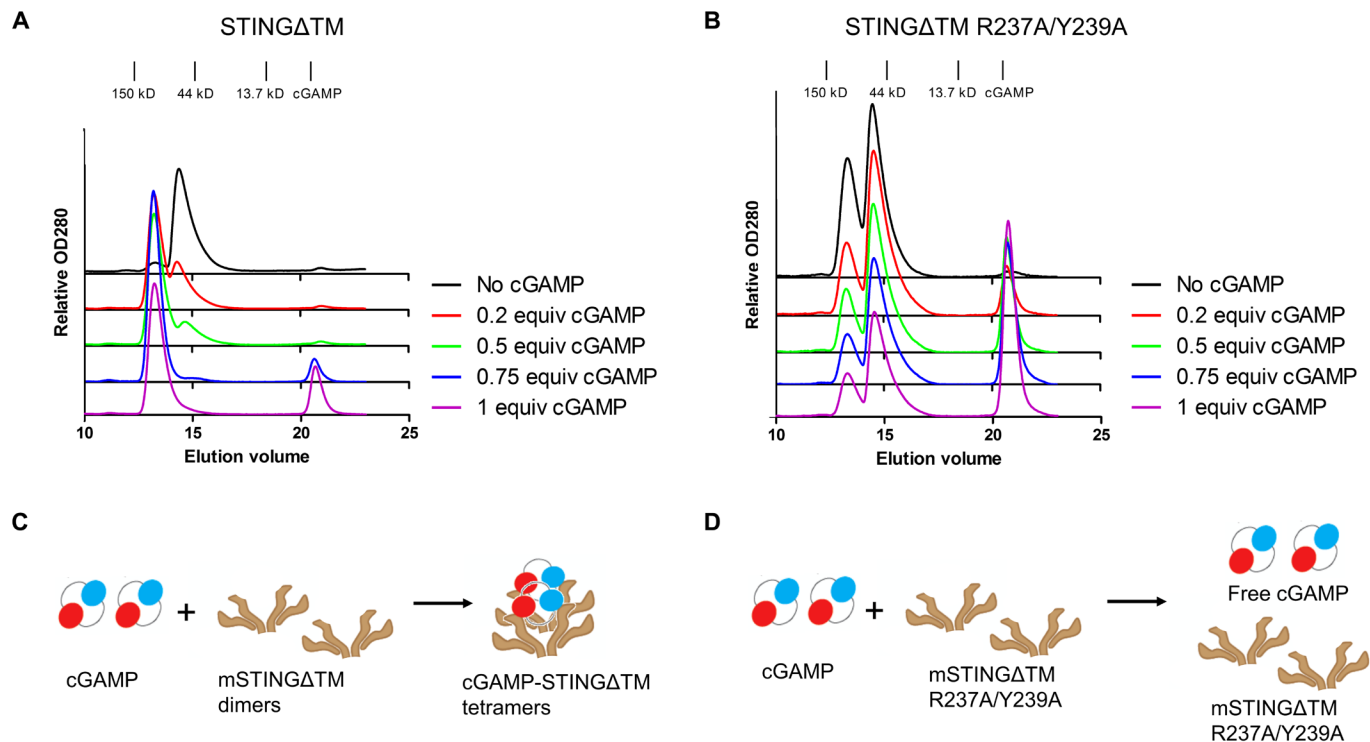
Fig. 2. cGAMP binding induces near-complete self-assembly of cGAMP-STINGΔTM tetramer. FPLC analyses of (**A**) mouse STINGΔTM and (**B**) R237A/Y239A mutant in PBS, titrated with various molar ratios of cGAMP and schematics of cGAMP-STINGΔTM tetramer self-assembly with (**C**) mouse STINGΔTM and (**D**) R237A/Y239A mutant, which is not capable of binding cGAMP.

Additional experiments were conducted with functional double mutants at the tetramer interface (Q272A/A276Q in mouse STINGΔTM) (fig. S2C). These mutants have been reported to disrupt the oligomerization of chicken STING, as well as abolish translocation and puncta formation induced by cGAMP (20). Unexpectedly, we observed the formation of tetrameric structures in the presence of these mutations. While beyond the scope of discussion in this work, these results may raise the possibility of a cGAMP-induced ΔTM tetrameric structure distinct from the wild-type (WT) STING oligomers studied in literature (20, 23).

It has been reported that STING moves from the ER and aggregates via oligomerization of the cytosolic CTD following its activation by cGAMP. This aggregation is essential for the binding and phosphorylation of TBK1, which subsequently phosphorylates IRF3 and initiates the downstream pathway (18). Recent structural analyses of the STING-TBK1 protein complex revealed that because of geometric constraints, the S366 of STING cannot be phosphorylated by the same TBK1 dimer it is bound to; instead, it interacts with the kinase site of the neighboring TBK1. Hence, a minimum of two neighboring dimers—a tetrameric structure—is needed for successful signaling. It was also found that after full-length STING in cells binds cGAMP, they form side-by-side tetramers that could assemble into larger oligomers to facilitate this transphosphorylation (20). We observed that cells overexpressing STINGΔTM do not exhibit this clustering of STINGΔTM molecules upon addition of cGAMP; the protein is evenly distributed in the cytosol, as the N-terminal domain that modulates the translocation from the ER is missing. However, when we directly delivered the tetramerized STINGΔTM protein with cGAMP via a commercial transfection reagent into cells, we observed the clustering behavior of the STINGΔTM protein that is essential for

IFN signaling (Fig. 3F). This was corroborated by in vitro activation tests of STING signaling, the details of which are discussed in the following section. We therefore hypothesize that the cGAMP-STINGΔTM tetrameric signaling complex created in the preassembly process was the pivotal factor for successful IFN signaling in cells.

cGAMP-STINGΔTM results in enhanced type I IFN signaling in vitro

Unless otherwise specified, we used human STINGΔTM for all human embryonic kidney (HEK) 293T cell in vitro IFN activation tests and mouse STINGΔTM for all remaining studies. In the figure legends, all proteins delivered in vitro and in vivo (denoted as ΔTM or mutants such as S365AΔTM) are referred to as STINGΔTM proteins, and all cGAMP codelivery groups comprise 1:1 molar equivalents of cGAMP:STINGΔTM. To verify the signaling efficacy of the cGAMP-STINGΔTM tetramer, we first delivered them to a mouse macrophage cell line RAW264.7 that has endogenous STING expression. Overall, we observed that the vehicle-free groups elicited higher IFN expression than the groups with commercial transfection reagent and that in both groups, cGAMP codelivery with STINGΔTM resulted in higher IFN expression than cGAMP delivered alone (Fig. 3B). In the presence of endogenous STING, mutant versions of cGAMP-STINGΔTM (S365A and R237A/Y239A) are as effective as the WT protein, suggesting that S365A and R237A/Y239A mutants may act as chaperones to shuttle cGAMP into cells while utilizing endogenous WT STING for activation of STING signaling.

We then tested the efficacy of cGAMP-STINGΔTM tetramer in an IFN-luciferase reporter cell line HEK293T, which was deficient in endogenous STING expression but expresses other essential proteins
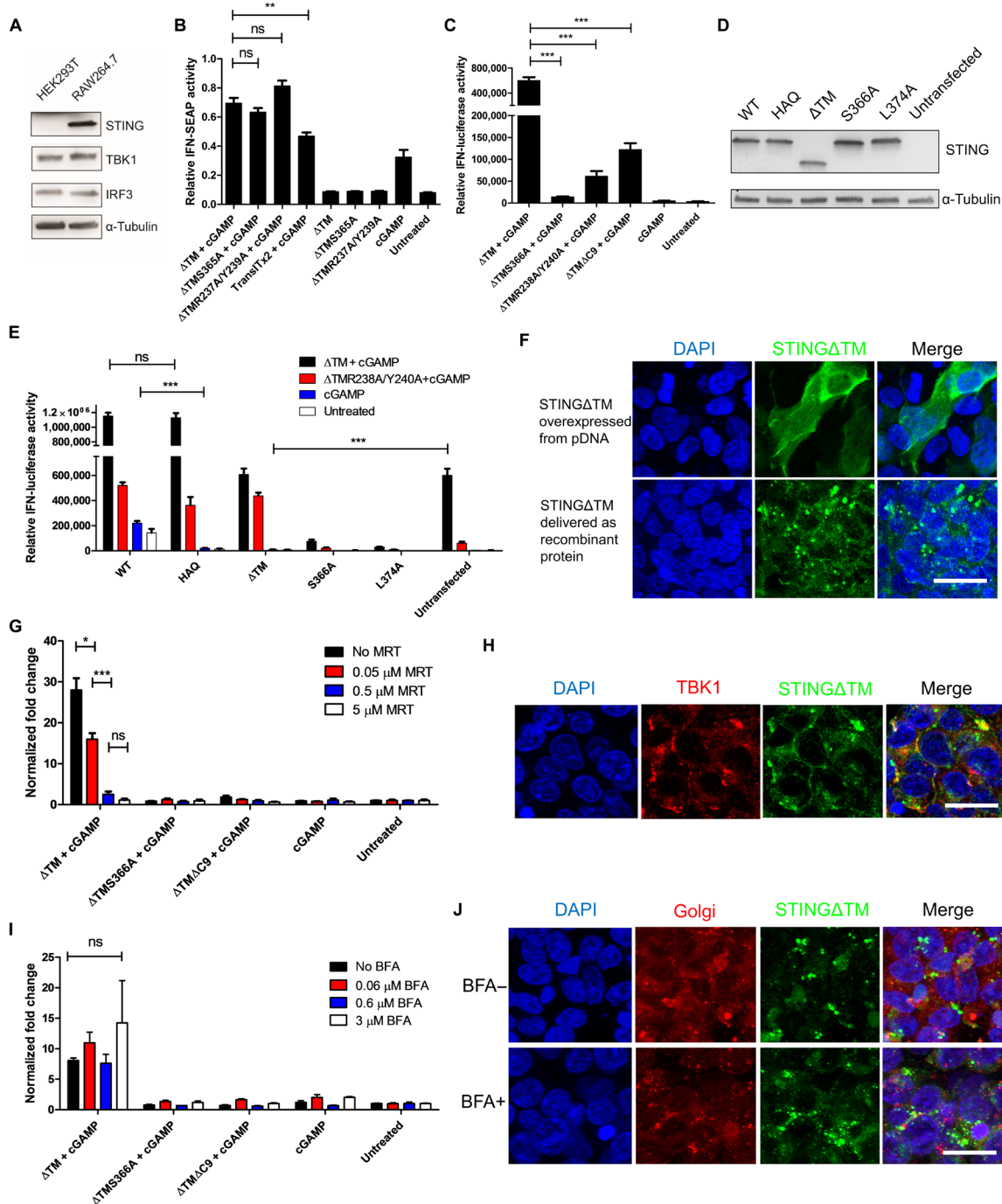
Fig. 3. cGAMP-STINGΔTM tetramer effectively triggers IFN expression in vitro, including in STING-deficient and STING-defective cell lines. (**A**) Immunoblotting of endogenous expression of STING, TBK1, and IRF3 in HEK293T and RAW264.7 cell line. (**B**) RAW264.7 cells ($n = 3$) and (**C**) HEK293T cells ($n = 4$) treated with different combinations/mutations of cGAMP-STINGΔTM tetramer (10 μg of STINGΔTM with 0.25 μg of cGAMP per milliliter). Luciferase and single enzyme activity–based protein profiling (SEAP) activity were determined 24 hours after treatment. (**D**) Immunoblotting of HEK293T cells transiently transfected with plasmid DNA overexpressing full-length human STING (WT, HAQ, S366A, and L374A) and hSTINGΔTM. (**E**) Transfected HEK293T cells ($n = 4$) in (D) treated with cGAMP-STINGΔTM tetramer (plus R238A/Y240A mutant), cGAMP only, and 10 μg of STINGΔTM with 0.25 μg of cGAMP per milliliter. Luciferase activity were determined 24 hours after treatment. (**F**) Confocal micrograph of HEK293T cells (upper) transfected with plasmid DNA encoding for STINGΔTM expression and then stimulated with cGAMP and (lower) with cGAMP-STINGΔTM tetramer delivered as ribonucleoprotein complex. (**G**) HEK293T cells ($n = 4$) pretreated with TBK1 inhibitor MRT67307 (MRT) and then treated with different combinations/mutations of cGAMP-STINGΔTM tetramer. (**H**) Confocal micrograph of HEK293T cells treated with cGAMP-STINGΔTM tetramer showing colocalization of STINGΔTM and TBK1. (**I**) HEK293T cells ($n = 4$) pretreated with BFA, which blocks ER-Golgi trafficking and then treated with different combinations/mutations of cGAMP-STINGΔTM tetramer. (**J**) Confocal micrograph of HEK293T cells ($n = 4$) treated with cGAMP-STINGΔTM tetramer showing no colocalization of STINGΔTM with Golgi apparatus, in the presence or absence of BFA. Values are reported as means ± SEM. ***$P < 0.001$, **$P < 0.01$, and *$P < 0.05$, as analyzed by one-way analysis of variance (ANOVA). Scale bars, 50 μm. ns, not significant.

for the STING signaling pathway including TBK1 and IRF3 (Fig. 3A). We generated this cell line by integrating an IFN-stimulated response element (ISRE) that drives the expression of luciferase in HEK293T cells. In addition, we included three functional STINGΔTM mutants: S366A, R238A/Y240A, and ΔC9 (deleting nine amino acids from the C-terminal tail), which are known to abrogate STING phosphorylation, cGAMP binding, and TBK1 binding, respectively (17), and confirmed that the STINGΔTM protein is indeed functional in triggering the STING pathway independent of endogenous STING (Fig. 3C).

Although the axes of Fig. 3 (B and C) are not directly comparable due to the use of two different IFN reporters (raw ISG blue for the RAW264.7 cell line and luciferase for the HEK293T cell line), it is apparent that in both cases, IFN activity is increased via the codelivery of cGAMP with STINGΔTM. And while there visually appears to be a far larger difference in IFN activity between the cGAMP and STINGΔTM plus cGAMP group in the HEK293T system, this is due to the lack of endogenous STING in the HEK293T cell line, leading to a negligible amount of IFN activity. Conversely, this difference is less pronounced in the RAW264.7 system due to the presence of endogenous STING, which leads to measurable IFN–secreted embryonic alkaline phosphatase (SEAP) activity in the cGAMP-only group (as it is able to function with endogenous STING).

We also evaluated the IFN activity of additional small-molecule agonists using cdiGMP and cGAM(PS)$_2$, a synthetic, nondegradable cGAMP analog, as previously described in the HEK293T system (fig. S4A). The system exhibited behavior similar to that of the cGAMP plus STINGΔTM codelivery group, namely, that the codelivery of STINGΔTM with these agonists resulted in increased IFN activity relative to all functional mutants tested and agonist-only controls. These studies suggest that the recombinant protein STINGΔTM-mediated enhanced type I IFN signaling derives from the preassembly of agonist and STINGΔTM and is independent of cell type or CDN species.

Last, we used several chemical inhibitors including MRT67307 (MRT), brefeldin A (BFA), chloroquine (CQ), and bafilomycin A1 (BafA1) to comprehensively dissect the intracellular trafficking of the tetrameric complex through confocal microscopy and quantification of IFN activity: At 6 hours after transfection, we observed limited colocalization of STINGΔTM with early endosome antigen 1 (EEA1), an early endosome marker, suggesting the potential escape of the early endosome into the cytosol (fig. S3B). IFN activity was observed to decrease with increasing concentrations of MRT (TBK1 inhibitor), which indicates that the STING signaling does proceed via a TBK1-dependent pathway (Fig. 3G). In addition, confocal microscopy images (also taken 6 hours after transfection) confirmed the colocalization of TBK1 with STINGΔTM in punctate structures that resemble those formed by cGAMP-activated full-length STING (Fig. 3H) (1). Interactions with IRF3 have previously been shown by coimmunoprecipitation of STINGΔTM with phosphorylated IRF3 (17). The presence of BFA, an inhibitor of ER-Golgi protein trafficking previously shown to block the full-length STING-induced IRF pathway (24, 25), appeared to have an insignificant effect on STINGΔTM-induced STING signaling (Fig. 3I). This was corroborated by no significant evidence of STINGΔTM colocalization with the Golgi apparatus with or without the addition of BFA (Fig. 3J), a markedly different phenomenon from literature reports of full-length STING localization with ERGIC (ER-Golgi intermediate compartment) disruptors (24, 26).

Another departure from similar assays on full-length STING was observed upon treatment of the cells with BafA1, an autophagy inhibitor. IFN activity was found to be significantly dependent on the concentration of BafA1, with decreasing activity observed with increasing concentrations of BafA1 (fig. S3A), which could suggest the necessity of autophagosome-lysosome fusion in STINGΔTM-induced STING signaling. The eventual degradation of STINGΔTM via a lysosomal pathway was observed in its colocalization with lysosomal-associated membrane protein 1 (LAMP1) at 24 hours after transfection, which was not apparent at 6 hours after transfection (fig. S3D). This was consistent with the increased IFN activity observed upon incubation with increasing concentrations of CQ (an inhibitor of lysosomal enzymes) (fig. S3C), as had been reported in literature with full-length STING (27).

While in the literature there are mixed reports on HAQ sensitivity to STING agonists relative to WT STING (10–15, 18), we set out to assess whether the codelivery of STINGΔTM and cGAMP can enhance IFN in HAQ-transfected cells in comparison to cGAMP-only treatment in HEK293T cells, which lack endogenous STING. HEK293T cells were transiently transfected with plasmid DNA encoding a full-length human STING (WT, 1 to 379 amino acids) or the HAQ allele, as a means to simulate cells with fully functioning STING and defective STING. Meanwhile, S366A (1 to 379 amino acids), L374A (1 to 379 amino acids), and STINGΔTM (139 to 379 amino acids) were also expressed separately in 293T as negative controls (Fig. 3D). Those cells with various defective STINGs were then treated with cGAMP-STINGΔTM tetramers, cGAMP mixed with STINGΔTM (R238A/Y240A), or cGAMP only. As shown in Fig. 3E, cells overexpressing HAQ STING were significantly less responsive to conventional cGAMP administration than cells expressing WT STING. Cells overexpressing STINGΔTM also did not result in significant IFN activity upon delivery of cGAMP only, a phenomenon previously reported in literature (1, 28, 29). However, when cGAMP was delivered in the form of cGAMP-STINGΔTM tetramers, both cells overexpressing HAQ STING and WT STING showed equally high levels of IFN expression. Increased IFN expression was also observed in cells overexpressing STINGΔTM. Untransfected cells likewise exhibited significantly higher IFN activity upon codelivery of the cGAMP-STINGΔTM tetramers when compared with cGAMP-only controls in untransfected cells and cells overexpressing WT STING. Therefore, we demonstrated that our method could potentially address the issue of STING heterogeneity in humans through the codelivery of cGAMP with a functional STINGΔTM carrier.

To conclude the in vitro characterization of our STINGΔTM-cGAMP tetrameric complex, we evaluated the expression of IFN-β, TBK1, and IRF3 in RAW264.7 and DC2.4 cell lines via quantitative polymerase chain reaction (qPCR), as a means of better understanding the effect of the delivery system on STING signaling intermediates (fig. S5). At 6 hours after treatment with cGAMP-STINGΔTM, we were able to observe a slight enhancement in TBK1, but not in IRF3 expression. Overall, delivery of cGAMP-STINGΔTM significantly increased the expression of IFN-β relative to cGAMP-only and STINGΔTM-only controls in both cell lines tested, demonstrating the capability of the system to achieve enhanced STING signaling in the presence of endogenous STING.

cGAMP-STINGΔTM induces dendritic cell maturation and strong humoral and cellular immune responses in vivo

To explore its application to boost the adjuvanticity potential of STING agonists (e.g., cGAMP), we first confirmed the influence of

cGAMP-STINGΔTM on dendritic cell maturation in vitro and in vivo. In brief, we analyzed the expression of IFN-β in dendritic cells 6 hours after treatment with cGAMP-STINGΔTM and found a significant increase in expression levels relative to cGAMP only and STINGΔTM controls. We were, likewise, able to confirm the effect of the tetramers on dendritic cell maturation in vivo following the treatment of C57BL/6 mice, where we observed significant up-regulation of the dendritic cell maturation marker major histocompatibility complex (MHC)–II$^+$ in CD11c$^+$ cells in the cGAMP-STINGΔTM trial compared with STINGΔTM and naïve controls (Fig. 4, A and B).

We then evaluated the humoral immune response elicited against ovalbumin (OVA) antigens with or without the STING-cGAMP adjuvant. Five groups of C57BL/6 mice were immunized on day 0 and boosted on day 7 with 10 µg of OVA alone or OVA mixed with 2.5 µg of cGAMP and/or 100 µg of STINGΔTM via tail base injection, as illustrated in Fig. 4C. On days 14, 28, and 42, sera were collected for enzyme-linked immunosorbent assay (ELISA) to determine the anti-OVA total immunoglobulin G (IgG) level. The groups vaccinated with the combination of OVA, cGAMP, and STINGΔTM generated a significantly more robust and sustained total IgG-based antigen-specific immune response compared with other control groups (Fig. 4, D to F). Additional experiments also demonstrated that no systemic toxicity occurred from tetramer delivery (fig. S6), specifically that there was no significant increase in the level of inflammatory cytokines [interleukin-6 (IL-6) and TNF-α] when compared with the injection of PBS. Release of cGAMP-STINGΔTM from the tail base was also sustained for over a week, with trafficking to the draining (inguinal) lymph nodes (fig. S7) that was 20- to 50-fold higher than in either STINGΔTM-only or cGAMP-only controls.

We then quantified the antigen-specific T cell activation via tetramer and intracellular cytokine staining of peripheral blood mononuclear cells (PBMCs) (30). Groups of C57BL/6 mice were immunized on day 0 and boosted on day 7 via tail base injection with 50 µg of OVA alone or OVA mixed with 1 µg of cGAMP and/or 40 µg of STINGΔTM (or 40 µg of S365A STINGΔTM). On day 14, mice were bled and PBMCs were separated from the whole blood (Fig. 5A). For tetramer staining, PBMCs were stained with anti-CD8
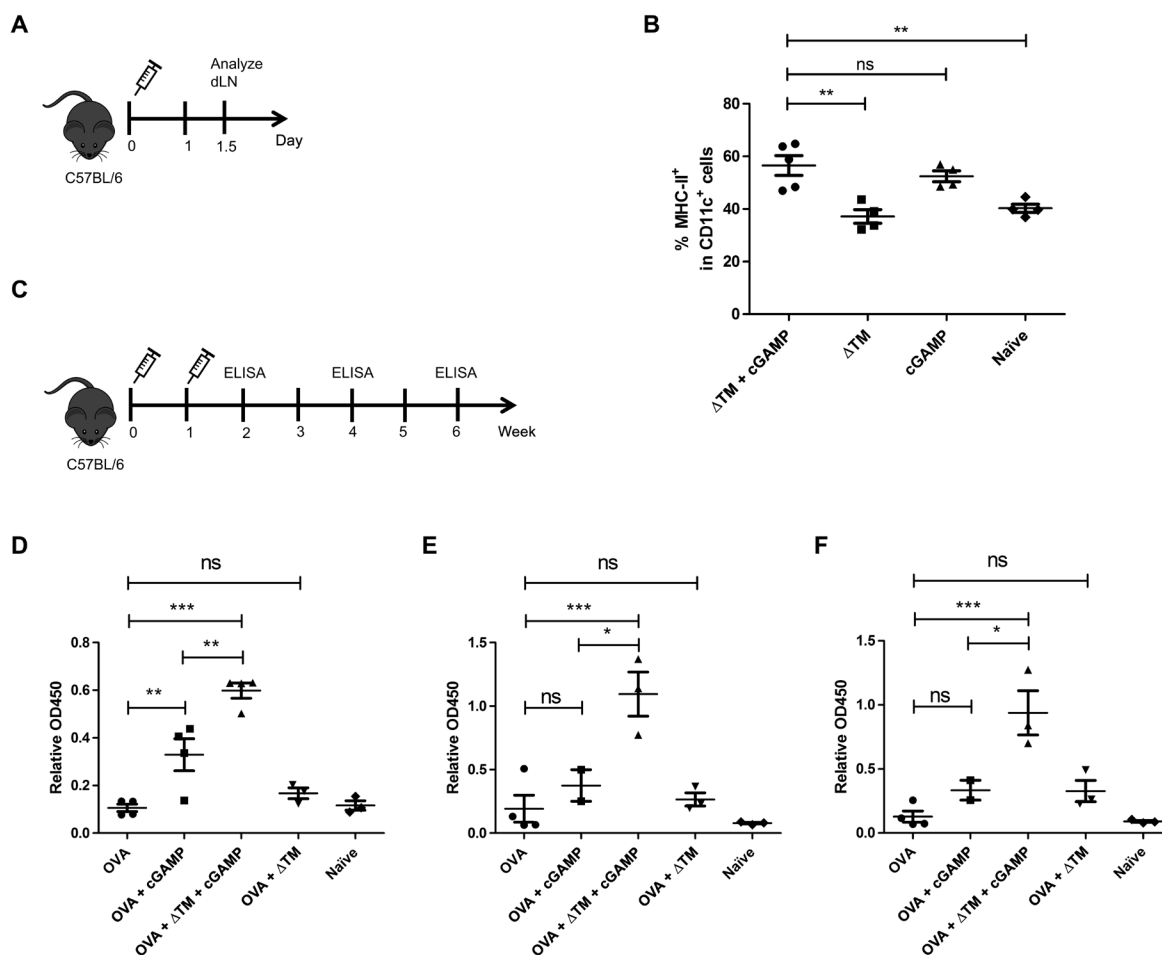
Fig. 4. cGAMP-STINGΔTM tetramer activates dendritic cells and promotes potent humoral response. (**A**) Groups of C57BL/6 mice ($n = 4$) were tail base injected with 40 µg of STINGΔTM, with or without 1 µg of cGAMP, or 1 µg of cGAMP alone on day 0, and then on day 1.5, draining (inguinal) lymph node lymphocytes were collected for analysis by flow cytometry. (**B**) Dendritic cell activation in draining (inguinal) lymph node gated by % MHC-II$^+$ cells in CD11c$^+$ cells. (**C**) C57BL/6 mice ($n = 4$) were immunized with 10 µg of ovalbumin (OVA) alone or OVA mixed with 2.5 µg of cGAMP or 100 µg of STINGΔTM or both via tail base injection on days 0 and 7. On days 14 (**D**), 28 (**E**), and 42 (**F**), OVA-specific total immunoglobulin G (IgG) antibody level in mouse serum was measured via enzyme-linked immunosorbent assay (ELISA). In (E) and (F), five mice were lost because of accidental cage flooding. Values are reported as means ± SEM. ***$P < 0.001$, **$P < 0.01$, and *$P < 0.05$, as analyzed by one-way ANOVA.
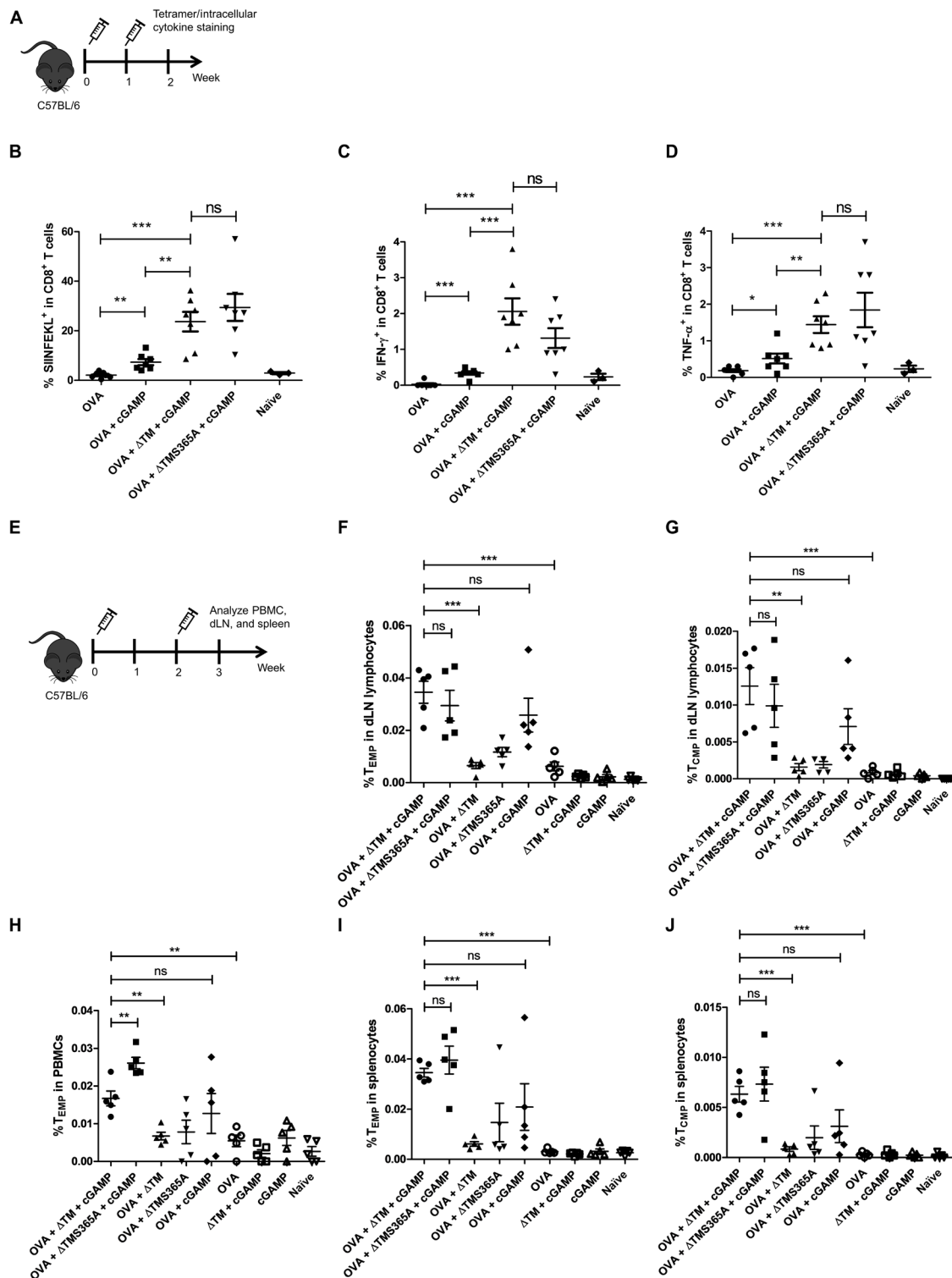
Fig. 5. cGAMP-STINGΔTM tetramer promotes robust antigen-specific T cell responses. (**A**) Groups of C57BL/6 mice (*n* = 7) were immunized with 50 μg of OVA alone or OVA mixed with 1 μg of cGAMP or 40 μg of STINGΔTM (or 40 μg of S365A STINGΔTM) on days 0 and 7. On day 14, PBMCs were collected and CD8$^+$ T cells were analyzed by CD8 OVA epitope SIINFEKL tetramer staining (**B**) or stimulated ex vivo with CD8 OVA epitope SIINFEKL and analyzed by intracellular cytokine staining of IFN-γ (**C**) and TNF-α (**D**). (**E**) Groups of C57BL/6 mice (*n* = 5) were immunized with 50 μg of OVA alone or OVA mixed with 1 μg of cGAMP or 40 μg of STINGΔTM (or 40 μg of S365A STINGΔTM) on days 0 and 14. On day 21, PBMCs and lymphocytes in dLN and splenocytes were collected and CD8$^+$ T cells were analyzed by CD8 OVA epitope SIINFEKL tetramer staining. Among CD8$^+$ SIINFEKL tetramer$^+$ T cells, effector memory precursors T$_{EMP}$ were gated by CD27$^+$ CD62L$^-$ and KLRG1$^-$ [(**F**) in dLN lymphocytes, (**H**) in PBMCs, and (**I**) in splenocytes], and central memory precursors T$_{CMP}$ were gated by CD27$^+$ CD62L$^+$ and KLRG1$^-$ [(**G**) in dLN lymphocytes and (**J**) in splenocytes, T$_{CMP}$ was generally not found in PBMCs]. Values are reported as means ± SEM. ***P < 0.001, **P < 0.01, and *P < 0.05, as analyzed by one-way ANOVA.
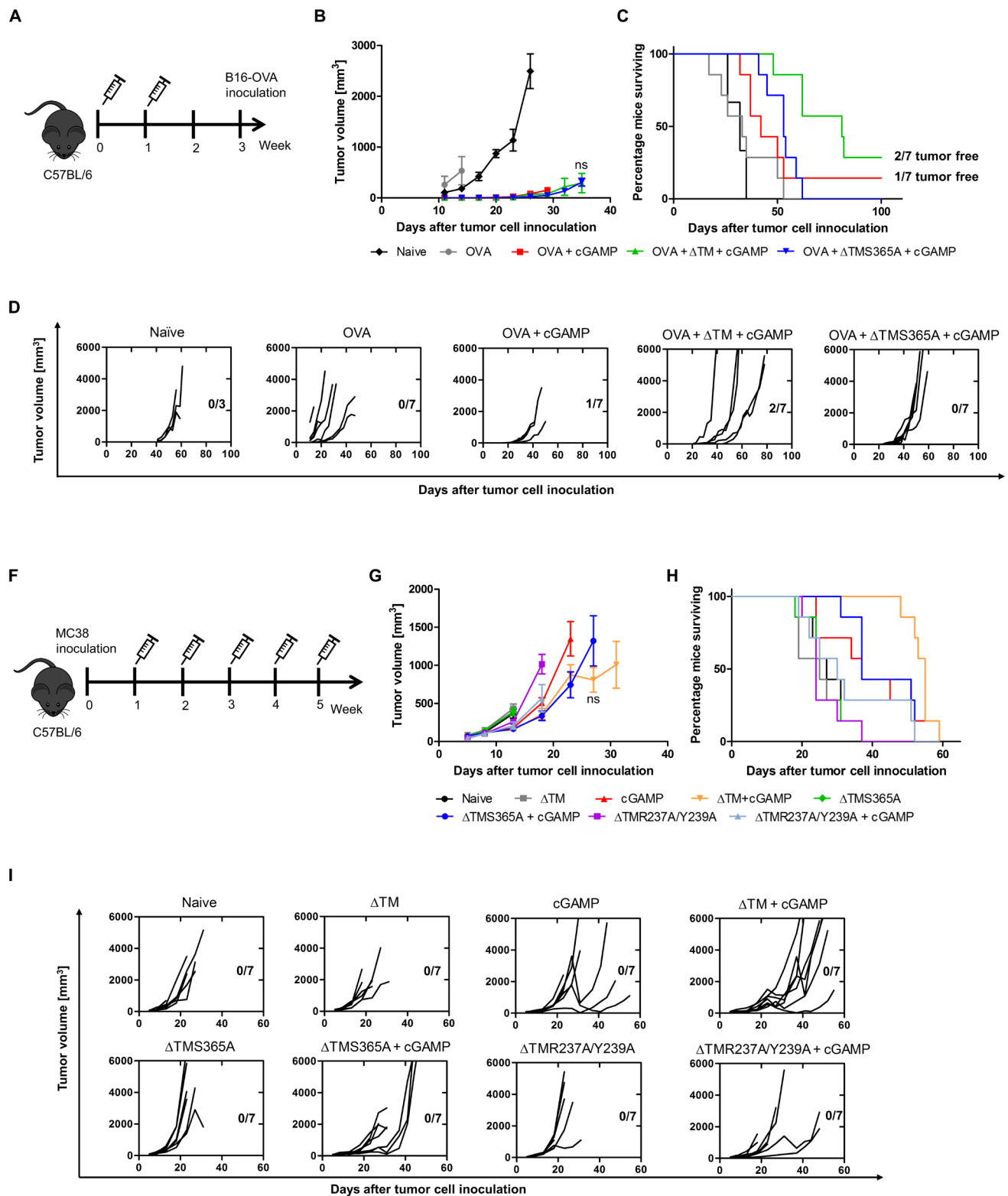
Fig. 6. cGAMP-STINGΔTM tetramer promotes potent antitumor immunity in B16 melanoma model. (**A**) Groups of C57BL/6 (*n* = 7) mice were immunized with 50 μg of OVA alone or OVA mixed with 1 μg of cGAMP or 40 μg of STINGΔTM (or 40 μg of S365ASTINGΔTM) on days 0 and 7. On day 21, mice were challenged with 1 million B16-OVA cells subcutaneously. Plots of overall (**B**) and individual (**D**) tumor growth curves, with numbers of surviving mice at the end of study (day 100) denoted. (**C**) Survival curves of mice. (**E**) Groups of C57BL/6 (*n* = 7) mice were first inoculated with 1 million MC38 cells and then treated with 100 μg of STINGΔTM (or 100 μg of S365A, R237A/Y239A STINGΔTM) mixed with 2.5 μg of cGAMP starting on day 7 for five times, 7 days apart via intratumoral injection. Plots of (**F**) overall and (**H**) individual tumor growth curves, with numbers of surviving mice at the end of study (day 60) denoted. (**G**) Survival curves of mice.

antibody and H-2K^b/SIINFEKL tetramer. For intracellular cyto-kine staining, cells were first stimulated with SIINFEKL peptide. They were then stained with anti-CD8 antibody and permeabilized for intracellular cytokine staining of TNF-α and IFN-γ. Figure 5 (B to D) shows that antigen delivered with both STINGΔTM and S365AΔTM plus cGAMP significantly increased the percentage of SIINFEKL$^+$ and both TNF-α− and IFN-γ−secreting CD8$^+$ T cells, which indicates that the tetramers resulted in successful IFN in-duction in T cells and is consistent with our in vitro STING signal-ing activation tests with RAW264.7 cells. Representative flow plots with gating strategies are shown in fig. S8.

Last, we investigated the induction of memory T cell response through the use of model antigen OVA. Groups of C57Bl/6 mice were immunized on day 0 and boosted on day 14 via tail base injec-tion with 50 μg of OVA alone or OVA mixed with 1 μg of cGAMP and/or 40 μg of STINGΔTM (or 40 μg of S365A STINGΔTM) (Fig. 5E). On day 21, mice were euthanized to harvest lymphocytes from the draining lymph nodes (dLN, inguinal) and splenocytes. As shown in Fig. 5 (F to J), the delivery of cGAMP-STINGΔTM resulted in the significant enhancement of SIINFEKL-specific central mem-ory T cell precursors (CD8$^+$, SIINFEKL$^+$, CD27$^+$, CD62L$^+$, and KLRG1$^-$) and effector memory T cell precursors (CD8$^+$, SIINFEKL$^+$, CD27$^+$, CD62L$^-$, and KLRG1$^-$) (31).

cGAMP-STINGΔTM enhances the antitumor therapeutic efficacy

To explore the potential of cGAMP-STINGΔTM tetramer as a new mode of STING agonist–based cancer immunotherapy, we first evaluated the antitumor efficacy of cGAMP-STINGΔTM tetramers with a prophylactic study, using a melanoma cell line modified to express SIINFEKL peptide (B16-OVA) as an antigen epitope for vaccination. Groups of animals from the tetramer and intracellular cytokine staining study were challenged with 1 million B16-OVA cells at day 21 via subcutaneous injection (Fig. 6A). Tumor sizes were measured every 3 days to monitor the cancer progression and were recorded before the death of any mouse within a group. Hence, antitumor therapeutic efficacy was evaluated from both tumor vol-ume (Fig. 6B) and mouse survival (Fig. 6, C and D). Groups vacci-nated with cGAMP plus OVA, cGAMP plus S365AΔTM plus OVA, and cGAMP plus ΔTM plus OVA showed significantly enhanced protection against tumor challenge compared with the untreated and OVA-only control groups (Fig. 6B). Among these groups, cGAMP plus ΔTM plus OVA exhibited the slowest tumor progres-sion and most prolonged survival, with two of seven mice achieving total protection and remaining tumor free (Fig. 6, C and D). The cGAMP plus S365AΔTM plus OVA group was also observed to re-sult in improved survival when compared with the cGAMP plus OVA group. The vaccination efficacy is consistent with the IFN-γ and TNF-α expression level observed in the intracellular cytokine staining.

We then performed a therapeutic treatment study with an MC38 colon cancer model. C57BL/6 mice were inoculated with 1 million MC38 cells subcutaneously on day 0. After the primary tumor was established (between 50 and 80 mm^3), 100 μg of STINGΔTM (plus S365A, or R237A/Y239A) with or without 2.5 μg of cGAMP was injected intratumorally on days 7, 14, 21, 28, and 35 (Fig. 6E). The tumor size and survival were monitored on a schedule similar to that of the prophylactic study. Treatment with cGAMP, cGAMP plus S365AΔTM, and cGAMP plus ΔTM significantly reduced tumor

burden, with the cGAMP plus ΔTM group having the overall best therapeutic effect and most prolonged survival (Fig. 6, F to H).

DISCUSSION

Numerous studies have suggested that the TM domain of STING protein is essential for intracellular STING signaling. Indeed, a STING-deficient cell line overexpressing TM-deficient STING will not undergo STING signaling upon free cGAMP delivery. However, we have found an interesting and well-defined self-assembled te-trameric structure of the TM-deficient STING protein with cGAMP under physiological conditions and found that when delivered to the cell, this ribonucleoprotein complex could effectively trigger the STING signaling pathway independent of the status of endogenous STING. While already confirmed through size exclusion chroma-tography, these tetramers could be further characterized via elec-trophoresis and ultracentrifugation in later studies. Ultimately, we developed this approach as a bioinspired method for cGAMP ther-apeutics to introduce a highly effective means of cGAMP delivery that potentially addresses the occurrence of defective STING in hu-mans either due to cancer epigenetics or genetic heterogeneity. In the interest of translational relevance, we tested the therapeutic effi-cacy of the platform in vivo and found that the cGAMP-STINGΔTM tetramers can promote robust humoral response and antigen-specific T cell activation and elicit superior antitumoral immunity against a melanoma and a colon cancer model. In light of the role of activat-ing STING signaling toward overcoming resistance against im-mune checkpoint blockade, future work can explore the delivery of cGAMP-STINGΔTM tetramers in combination with antiPD(L)1 and anti-CTLA4. Alternatively, genetic fusion of STINGΔTM tetramers with tumor-specific antigen peptides may enable simulta-neous delivery of STING agonist–based adjuvant and antigens into dendritic cells to maximize the immune response. In summary, this work may open a new paradigm toward engineering immune adap-tors to address vaccinology and immunotherapy.

MATERIALS AND METHODS
STINGΔTM protein purification
The STINGΔTM protein of mouse (138 to 378 amino acids) and human (139 to 379 amino acids) were synthesized by gBlock (IDT) and cloned into pSH200 plasmid (a gift from X. Shen at Duke Uni-versity) via Nco I and Not I. Mutants were created by site-specific mutagenesis based on the plasmids encoding for STINGΔTM (primers listed in table S1). His-tagged STINGΔTM protein was expressed in DE3 *Escherichia coli* (mSTING ΔTM in BL21 DE3, hSTINGΔTM in Rosetta DE3), cultured at 37°C until OD600 reaches 0.4, and then induced with 0.5 mM isopropyl-β-D-thiogalactopyranoside (IPTG) at 18°C overnight. After induction, cells were centrifuged and lysed at room temperature for 20 min in protein binding buffer (50 mM sodium phosphate, 0.5 M NaCl, and 10 mM imidazole) with 1% Triton X-100 and lysozyme (1 mg/ml) and sonicated at 18 W (with 3-s on and 5-s off intervals) for a total of 5 min on ice. Cell lysate was then centrifuged at 14,000g, 4°C for 30 min and incubated with cobalt beads (HisPur Cobalt Resin; Thermo Fisher Scientific, 89964) followed by washing (50 mM sodium phosphate, 0.5 M NaCl, 10 mM imidazole, and 0.1% Triton X-114), elution (50 mM sodium phos-phate, 0.5 M NaCl, and 150 mM imidazole), and desalting (buffer exchange to 20 mM Hepes, 150 mM NaCl, 10% glycerol, and 1 mM

DTT). Protein concentration was determined by bicinchoninic acid (BCA) assay, and protein purity was verified by SDS–polyacrylamide gel electrophoresis (SDS-PAGE) and FPLC.

FPLC characterization of cGAMP-STINGΔTM complex

The ribonucleoprotein complexes of cGAMP-STINGΔTM (and R237A/Y239A, Q272A/A276Q mutants) were analyzed using an AKTA pure FPLC. Three hundred micrograms of protein in 0.5 ml of PBS with various molar ratios of cGAMP was first mixed and incubated at room temperature for 30 min. The sample was injected into 10 ml of superloop and then loaded onto a Superdex 200 Increase 10/300 GL column (column volume of 23.56 ml) followed by isocratic elution of 1.25 column volume with PBS at 1 ml/min flow rate. The protein concentration was monitored with OD280. A fraction collector was used to collect 0.5 ml of fractions for SDS-PAGE analyses (fig. S2, A and B).

Cell culture

HEK293T cells were obtained from the American Type Culture Collection (ATCC; Rockville, MD, USA) and cultured in Dulbecco's modified Eagle's medium (DMEM) (Invitrogen) with 10% fetal bovine serum (FBS) and 1% penicillin/streptomycin. Nuclear factor κB (NF-κB) Reporter RAW264.7 (RAW-Blue cells) were obtained from InvivoGen and cultured in DMEM with 10% heat-inactivated FBS and 1% penicillin/streptomycin. All cell lines were used at low passage number and tested negative for *Mycoplasma* contamination.

In vitro STING signaling activation assays

RAW-Blue cells were seeded in 96-well plates at 3×10^5 cells/ml in 100 μl of DMEM with 10% heat-inactivated FBS and 1% penicillin/streptomycin per well. After 24 hours of incubation, 5 μg of mSTING ΔTM protein (or mutants) with 0.125 μg of cGAMP premixed and equilibrated in 20 μl of Opti-MEM media was added to each well and incubated overnight. After incubation, 20 μl of the induced RAW-Blue cell supernatant was added to 180 μl of QUANTI-Blue solution per well of a 96-well plate. The plate was incubated in 37°C for 6 to 10 hours until a visible color difference was observed. IFN-SEAP activity was then determined by the absorbance at 635 nm with a spectrophotometer.

For the HEK293T cells, we first generated a reporter derivative from this cell line by transfecting pGL4.45[luc2P/ISRE/Hygro] (Promega) and stably selected in hygromycin (200 μg/ml). The pGL4.45[luc2P/ISRE/Hygro] vector contains five copies of an ISRE that drives transcription of the luciferase reporter gene luc2P (*Photinus pyralis*). luc2p is a synthetically derived luciferase sequence with humanized codon optimization that is designed for high expression and reduced anomalous transcription. The luc2P gene contains hPEST, a protein destabilization sequence, which allows luc2P protein levels to respond more quickly than those of luc2p to induction of transcription. The cells were seeded in six-well plates at 3×10^5 cells/ml in 2.5 ml of DMEM with 10% FBS and 1% penicillin/streptomycin. After an overnight incubation, the cells were transiently transfected with plasmids (a gift from L. Jin, University of Florida) encoding for expression of full-length hSTING (1 to 379 amino acids) WT, HAQ, S366A, and L374A, plus the TM domain–deficient hSTING (139 to 379 amino acids). Commercial transfection reagent TransIT-X2 was used to help transfection (2 μg of plasmid DNA mixed with 4 μl of TransIT-X2 in 250 μl of Opti-

MEM media for each six well). The following day, cells were redistributed into 96-well plates at a seeding density of 3×10^5 cells/ml in 100 μl of media per well to be treated with cGAMP-STINGΔTM after 24 hours of incubation [2 μg of protein with or without 0.05 μg of CDNs cGAMP, cGAM(PS)$_2$, or cdi-GMP per well, with the help of 4 μl of TransIT-X2]. For assays with chemical inhibitors, HEK293T cells were treated with TBK1 inhibitor MRT67307 (InvivoGen, catalog no. inh-mrt; 6 hours before cGAMP-STINGΔTM treatment), CQ (Enzo, catalog no. 51005-CLQ; 2 hours before cGAMP-STINGΔTM treatment), BafA1 (InvivoGen, catalog no. tlrl-baf1; 2 hours before cGAMP-STINGΔTM treatment), and BFA (InvivoGen, catalog no. inh-bfa; 2 hours before cGAMP-STINGΔTM treatment). Transfected cells were also harvested for Western blotting.

Western blotting

Cells were washed with PBS and collected in T-PER tissue protein extraction reagent (30 μl per million cells) with Halt protease and phosphatase inhibitor cocktail (Thermo Fisher Scientific, no. 78442). The cells were lysed at 4°C for 30 min and centrifuged at 14,000g for 10 min. The protein concentration in the supernatant was determined via BCA assay, and SDS-PAGE samples were prepared as 50 μg of total protein in 30 μl of SDS-PAGE loading buffer. Anti-TBK1 (Cell Signaling, no. 3504), anti-STING (Novus Biologicals, NBP2-24683), anti–β-actin (Cell Signaling), and anti-tubulin (Cell Signaling).

Quantification of STING signaling–associated protein expression by qPCR

Total RNA was extracted using RNeasy micro kit (Qiagen, 74004) and reverse transcribed to cDNA with reverse transcription kit (Thermo Fisher Scientific, 4374966). cDNA was amplified and quantified by a Roche LightCycler 480 real-time PCR system. qPCR primers used for detection are mTBK1-F:GACATGCCTCTCTCCT-GTAGTC, mTBK1-R:GGTGAAGCACATCACTGGTCTC, mIRF3-F: CGGAAAGAAGTGTTGCGGTTAGC, mIRF3-R:CAGGCTGCTTTTGC-CATTGGTG, mIFN-β-F:GCCTTTGCCATCCAAGAGATGC, and mIFN-β-R:ACACTGTCTGCTGGTGGAGTTC.

Immunocytochemistry

Transfection and immune staining were performed in Millicell EZ chamber slides (Millipore Sigma, Temecula, CA, USA). Cells were fixed by 4% formaldehyde in PBS for 15 min, permeabilized by 0.4% Triton X-100 on ice for 10 min, and stained with rabbit anti-STING antibody (1:400; Novus bio, NBP2-24683) overnight at 4°C, or in the case of cells transfected with FLAG-STINGΔTM, stained with Cy3-conjugated anti-FLAG antibody (Sigma, A9594). For recombinant STING, proteins were conjugated with NHS–Alexa Fluor 488 (Thermo Fisher Scientific). Other primary antibodies used are anti-TBK1 (Abcam, ab235253), anti-LAMP1 (Cell Signaling, 9091S), and anti-EEA1 (Cell Signaling, 3288S). After washing with PBS containing 0.05% Tween 20, cells were stained with secondary antibodies including Alexa Fluor 568–conjugated goat anti-rabbit IgG antibody (Thermo Fisher Scientific, no. A-11011) and Alexa Fluor 488–conjugated donkey anti-rabbit IgG antibody (Thermo Fisher Scientific, no. A-32790). Nuclei were counterstained with 4′,6-diamidino-2-phenylindole (DAPI) and Golgi apparatus was stained with Golgi-ID green detection kit (Enzo Life Sciences, 51028-GG). Cells were imaged with an inverted Olympus IX83 microscope

equipped with a Hamamatsu ImagEM high-sensitivity camera at the Swanson Biotechnology Center (MIT).

Mice and immunizations

C56BL/6 (B6), C57BL/6-Tg(TcraTcrb)1100Mjb/J (OT-1) mice were purchased from the Jackson laboratory and housed in the MIT Animal Facility. All mouse studies were performed according to the protocols approved by the MIT Division of Comparative Medicine. Experiments were conducted using female mice 8 to 12 weeks old. For immunizations performed with tail base injections, 50 μl was injected per side of the tail, 100 μl dosage total in PBS. Blood was collected via cheek bleeding, 100 to 150 μl of blood each time collected in 5 μl of 0.5 M EDTA at pH 8. For the humoral response experiments, B6 mice were immunized with 10 μg of OVA alone or OVA mixed with 2.5 μg of cGAMP and/or 100 μg of mSTING ΔTM or both on days 0 and 7. Sera were collected on a biweekly basis starting from day 14 for ELISA analyses of anti-OVA total IgG level. For the tetramer, intracellular cytokine staining, and B16 prophylactic study, groups of B6 mice received 50 μg of OVA or OVA mixed with 1 μg of cGAMP or plus 40 μg of mSTING (or S365A) ΔTM protein on days 0 and 7. On day 14, PBMCs were collected for tetramer and intracellular cytokine staining. For the memory T cell precursor study, B6 mice were immunized with the same dosage at day 0 as prime and day 14 as boost. On day 21, blood was collected via cheek bleeding, and dLN inguinal lymph nodes and spleens were harvested. Blood was processed in the same way to obtain PBMCs. For the in vivo dendritic cell activation study, B6 mice were immunized with the same dosage at day 0 and euthanized at day 1.5 to harvest for inguinal lymph nodes. For the systemic toxicity study, groups of B6 mice were bled before and 2 hours after tail base injections of 1 μg of cGAMP mixed with 2 μl of TransIT-X2 or 40 μg of mSTING dissolved in 100 μl of PBS or PBS only as control. ΔTM protein PBMCs of OT-1 mice were collected as a positive control for SIINFEKL-specific T cell activation. On day 21, mice were inoculated with 1 million B16-OVA cells subcutaneously in the right hind flank. For the MC38 treatment study, groups of B6 mice were inoculated with 1 million MC38 cells subcutaneously in the right hind flank on day 0 and then treated weekly with 100 μg of mSTING ΔTM protein (or S365A, R237A/Y239A) with or without 2.5 μg of cGAMP starting on day 7 for five times.

ELISA, intracellular cytokine staining, and tetramer staining

Blood collected were centrifuged at 500g for 3 min. Sera were removed for ELISA detection of IL-6 (R&D, catalog no. DY406), TNF-α (R&D, catalog no. DY410), and OVA-specific antibody levels. ELISA assays were made in-house by coating high-binding ELISA plate (Corning) with protein (OVA) (10 μg/ml) or capture antibody for mouse IL-6 and TNF-α in 50 mM sodium bicarbonate buffer (pH 9.6) overnight. On the next day, wells were washed with PBS followed by blocking with 1% BSA in PBS at room temperature (RT) for an hour. Diluted sera were added into wells and incubated at RT for 2 hours. Detection antibodies for IL-6 and TNF-α, or anti-mouse IgG, horseradish peroxidase–linked antibody (Cell Signaling, catalog no. 7076) was diluted in 1% BSA in PBS at 1:5000. Samples were washed extensively with 1x PBS containing 0.05% Tween 20 in between. TMB (BioLegend) was used as the substrate, and reaction was quenched by HCl. Plates were measured at optical density (OD) of 450 nm.

The blood cell pellet was lysed with red blood cell lysing buffer Hybri-Max (Sigma-Aldrich, R7757) and washed with PBS to obtain

PBMCs. Inguinal lymph nodes and spleens were first homogenized with frosted microscope slides and filtered through cell strainers in fluorescence-activated cell sorting buffer. Lymphocytes were then ready for staining. Splenocytes were processed with red blood cell lysis buffer before staining. For intracellular cytokine staining, the PBMCs were first stimulated by resuspending in 400 μl of RPMI media with 10% FBS, 0.1 mM nonessential amino acids, 50 μM β-mercaptoethanol, 1% penicillin/streptomycin, SIINFEKL peptide (1 μg/ml) (Anaspec Inc., AS-60193-1), and BD GolgiStop (4 μl of BD GolgiStop for every 6 ml) and incubated at 37°C for 4 hours. The PBMCs were then treated with Fc blocker (anti-mouse CD16/CD32 monoclonal antibodies) followed by viability staining (LIVE/DEAD fixable aqua stain; Thermo Fisher Scientific, L34965) and surface staining with anti-CD8 antibodies (BioLegend, 100707; clone 53-6.7). After the surface staining, the PBMCs were then fixed, permeabilized, and stained with anti-mouse IFN-γ (BioLegend, 505825; clone XMG1.2) and anti-mouse TNF-α (BioLegend, 506107; clone TN3-19.12) antibodies, and then analyzed on a BD FACSCanto flow cytometer. For tetramer staining, the PBMCs obtained from blood were, likewise, directly treated with Fc blocker, viability staining, and surface staining with anti-CD8 and H-2Kb/SIINFEKL tetramer, and then fixed with formalin. For the memory T cell precursor study, PBMCs, lymphocytes, and splenocytes were treated with Fc blocker, viability staining, and surface staining with anti-CD8, H-2Kb/SIINFEKL tetramer, anti-mouse CD27 (BioLegend, 124212, clone LG.3A10), anti-mouse KLRG1 (BioLegend, 138416, clone 2F1/KLRG1), and anti-mouse CD62L (BioLegend, 104436, clone MEL-14). For the dendritic cell maturation study, lymphocytes were treated with Fc blocker, viability staining, and surface staining with anti-mouse CD11c (BioLegend, 117310, clone N418) and anti-mouse MHC class II (BioLegend, 107606, clone M5/114.15.2). Stained cells were then washed and analyzed on a BD FACSCelesta and LSRFortessa flow cytometer.

In vivo imaging

Balb/c mice tail base injected (on both sides of the tail) with Cy7-NHS ester–labeled STINGΔTM-cGAMP complex, Cy7-labeled STINGΔTM, and Cy7-labeled cGAMP were imaged under isoflurane anesthesia with Xenogen IVIS system. Acquisition and analysis of images were performed with Living Image software (Xenogen).

Statistical analysis

All statistical analyses were performed using GraphPad Prism 5.03 (San Diego, CA, USA). Data were analyzed with one-way analysis of variance (ANOVA) followed by Student's t test for statistical significance.

REFERENCES AND NOTES

1. B. Zhao, F. du, P. Xu, C. Shu, B. Sankaran, S. L. Bell, M. Liu, Y. Lei, X. Gao, X. Fu, F. Zhu, Y. Liu, A. Laganowsky, X. Zheng, J.-Y. Ji, A. P. West, R. O. Watson, P. Li, A conserved PLPLRT/SD motif of STING mediates the recruitment and activation of TBK1. *Nature* **569**, 718–722 (2019).

2. S.-R. Woo, M. B. Fuertes, L. Corrales, S. Spranger, M. J. Furdyna, M. Y. K. Leung, R. Duggan, Y. Wang, G. N. Barber, K. A. Fitzgerald, M.-L. Alegre, T. F. Gajewski, STING-dependent cytosolic DNA sensing mediates innate immune recognition of immunogenic tumors. *Immunity* **41**, 830–842 (2014).

3. L. Corrales, S. M. McWhirter, T. W. Dubensky Jr., T. F. Gajewski, The host STING pathway at the interface of cancer and immunity. *J. Clin. Invest.* **126**, 2404–2411 (2016).

4. S. T. Koshy, A. S. Cheung, L. Gu, A. R. Graveline, D. J. Mooney, Liposomal delivery enhances immune activation by STING agonists for cancer immunotherapy. *Adv. Biosyst.* **1**, 1600013 (2017).

5. T. Ohkuri, A. Kosaka, K. Ishibashi, T. Kumai, Y. Hirata, K. Ohara, T. Nagato, K. Oikawa, N. Aoki, Y. Harabuchi, E. Celis, H. Kobayashi, Intratumoral administration of cGAMP transiently accumulates potent macrophages for anti-tumor immunity at a mouse tumor site. *Cancer Immunol. Immunother.* **66**, 705–716 (2017).

6. D. Shae, K. W. Becker, P. Christov, D. S. Yun, A. K. R. Lytton-Jean, S. Sevimli, M. Ascano, M. Kelley, D. B. Johnson, J. M. Balko, J. T. Wilson, Endosomolytic polymersomes increase the activity of cyclic dinucleotide STING agonists to enhance cancer immunotherapy. *Nat. Nanotechnol.* **14**, 269–278 (2019).

7. T. W. Dubensky Jr., D. B. Kanne, M. L. Leong, Rationale, progress and development of vaccines utilizing STING-activating cyclic dinucleotide adjuvants. *Ther. Adv. Vaccines* **1**, 131–143 (2013).

8. J. Ahn, H. Konno, G. N. Barber, Diverse roles of STING-dependent signaling on the development of cancer. *Oncogene* **34**, 5302–5308 (2015).

9. T. Xia, H. Konno, G. N. Barber, Recurrent loss of STING signaling in melanoma correlates with susceptibility to viral oncolysis. *Cancer Res.* **76**, 6747–6759 (2016).

10. L. Jin, L. G. Xu, I. V. Yang, E. J. Davidson, D. A. Schwartz, M. M. Wurfel, J. C. Cambier, Identification and characterization of a loss-of-function human MPYS variant. *Genes Immun.* **12**, 263–269 (2011).

11. S. Patel, S. M. Blaauboer, H. R. Tucker, S. Mansouri, J. S. Ruiz-Moreno, L. Hamann, R. R. Schumann, B. Opitz, L. Jin, The common R71H-G230A-R293Q human TMEM173 is a null allele. *J. Immunol.* **198**, 776–787 (2017).

12. S. Patel, L. Jin, TMEM173 variants and potential importance to human biology and disease. *Genes Immun.* **20**, 82–89 (2019).

13. J. S. Ruiz-Moreno, L. Hamann, J. A. Shah, A. Verbon, F. P. Mockenhaupt, M. Puzianowska-Kuznicka, J. Naujoks, L. E. Sander, M. Witzenrath, J. C. Cambier, N. Suttorp, R. R. Schumann, L. Jin, T. R. Hawn, B. Opitz; CAPNETZ Study Group, The common HAQ STING variant impairs cGAS-dependent antibacterial responses and is associated with susceptibility to Legionnaires' disease in humans. *PLOS Pathog.* **14**, e1006829 (2018).

14. S. Patel, S. M. Blaauboer, H. R. Tucker, S. Mansouri, J. S. Ruiz-Moreno, L. Hamann, R. R. Schumann, B. Opitz, L. Jin, Response to comment on "The common R71H-G230A-R293Q human TMEM173 is a null allele". *J. Immunol.* **198**, 4185–4188 (2017).

15. K. E. Sivick, N. H. Surh, A. L. Desbien, E. P. Grewal, G. E. Katibah, S. M. McWhirter, T. W. Dubensky Jr., Comment on "The Common R71H-G230A-R293Q Human TMEM173 Is a Null Allele". *J. Immunol.* **198**, 4183–4185 (2017).

16. J. Fu, D. B. Kanne, M. Leong, L. H. Glickman, S. M. McWhirter, E. Lemmens, K. Mechette, J. J. Leong, P. Lauer, W. Liu, K. E. Sivick, Q. Zeng, K. C. Soares, L. Zheng, D. A. Portnoy, J. J. Woodward, D. M. Pardoll, T. W. Dubensky Jr., Y. Kim, STING agonist formulated cancer vaccines can cure established tumors resistant to PD-1 blockade. *Sci. Transl. Med.* **7**, 283ra52 (2015).

17. Y. Tanaka, Z. J. Chen, STING specifies IRF3 phosphorylation by TBK1 in the cytosolic DNA signaling pathway. *Sci. Signal.* **5**, ra20 (2012).

18. G. Surpris, J. Chan, M. Thompson, V. Ilyukha, B. C. Liu, M. Atianand, S. Sharma, T. Volkova, I. Smirnova, K. A. Fitzgerald, A. Poltorak, Cutting edge: Novel Tmem173 allele reveals importance of STING N terminus in trafficking and type I IFN production. *J. Immunol.* **196**, 547–552 (2016).

19. C. Zhang, G. Shang, X. Gui, X. Zhang, X.-c. Bai, Z. J. Chen, Structural basis of STING binding with and phosphorylation by TBK1. *Nature* **567**, 394–398 (2019).

20. G. Shang, C. Zhang, Z. J. Chen, X.-c. Bai, X. Zhang, Cryo-EM structures of STING reveal its mechanism of activation by cyclic GMP–AMP. *Nature* **567**, 389–393 (2019).

21. M. C. Hanson, M. P. Crespo, W. Abraham, K. D. Moynihan, G. L. Szeto, S. H. Chen, M. B. Melo, S. Mueller, D. J. Irvine, Nanoparticulate STING agonists are potent lymph node–targeted vaccine adjuvants. *J. Clin. Invest.* **125**, 2532–2546 (2015).

22. X. Zhang, H. Shi, J. Wu, X. Zhang, L. Sun, C. Chen, Z. J. Chen, Cyclic GMP-AMP containing mixed phosphodiester linkages is an endogenous high-affinity ligand for STING. *Mol. Cell* **51**, 226–235 (2013).

23. S. Ouyang, X. Song, Y. Wang, H. Ru, N. Shaw, Y. Jiang, F. Niu, Y. Zhu, W. Qiu, K. Parvatiyar, Y. Li, R. Zhang, G. Cheng, Z.-J. Liu, Structural analysis of the STING adaptor protein reveals a hydrophobic dimer interface and mode of cyclic di-GMP binding. *Immunity* **36**, 1073–1086 (2012).

24. N. Dobbs, N. Burnaevskiy, D. Chen, V. K. Gonugunta, N. M. Alto, N. Yan, STING activation by translocation from the ER is associated with infection and autoinflammatory disease. *Cell Host Microbe* **18**, 157–168 (2015).

25. H. Ishikawa, Z. Ma, G. N. Barber, STING regulates intracellular DNA-mediated, type I interferon-dependent innate immunity. *Nature* **461**, 788–792 (2009).

26. B. Hiller, V. Hornung, STING Signaling the enERGIC Way. *Cell Host Microbe* **18**, 137–139 (2015).

27. D. Liu, H. Wu, C. Wang, Y. Li, H. Tian, S. Siraj, S. A. Sehgal, X. Wang, J. Wang, Y. Shang, Z. Jiang, L. Liu, Q. Chen, STING directly activates autophagy to tune the innate immune response. *Cell Death Differ.* **26**, 1735–1749 (2019).

28. D. L. Burdette, K. M. Monroe, K. Sotelo-Troha, J. S. Iwig, B. Eckert, M. Hyodo, Y. Hayakawa, R. E. Vance, STING is a direct innate immune sensor of cyclic di-GMP. *Nature* **478**, 515–518 (2011).

29. P.-H. Wang, S.-Y. Fung, W.-W. Gao, J.-J. Deng, Y. Cheng, V. Chaudhary, K.-S. Yuen, T.-H. Ho, C.-P. Chan, Y. Zhang, K.-H. Kok, W. Yang, C.-P. Chan, D.-Y. Jin, A novel transcript isoform of STING that sequesters cGAMP and dominantly inhibits innate nucleic acid sensing. *Nucleic Acids Res.* **46**, 4054–4071 (2018).

30. P. Giannetti, A. Facciabene, N. La Monica, L. Aurisicchio, Individual mouse analysis of the cellular immune response to tumor antigens in peripheral blood by intracellular staining for cytokines. *J. Immunol. Methods* **316**, 84–96 (2006).

31. Y. Li, C. Shen, B. Zhu, F. Shi, H. N. Eisen, J. Chen, Persistent antigen and prolonged AKT−mTORC1 activation underlie memory CD8 T cell impairment in the absence of CD4 T cells. *J. Immunol.* **195**, 1591–1598 (2015).

Citation: Y. He, C. Hong, E. Z. Yan, S. J. Fletcher, G. Zhu, M. Yang, Y. Li, X. Sun, D. J. Irvine, J. Li, P. T. Hammond, Self-assembled cGAMP-STING∆TM signaling complex as a bioinspired platform for cGAMP delivery. *Sci. Adv.* **6**, eaba7589 (2020).

Science Advances

Self-assembled cGAMP-STING∆TM signaling complex as a bioinspired platform for cGAMP delivery

Yanpu He, Celestine Hong, Emily Z. Yan, Samantha J. Fletcher, Ge Zhu, Mengdi Yang, Yingzhong Li, Xin Sun, Darrell J. Irvine, Jiahe Li, and Paula T. Hammond

View the article online
Permissions

Use of this article is subject to the Terms of service